Science and Technology of Welding and Joining

ISSN: 1362-1718 (Print) 1743-2936 (Online) Journal homepage: http://www.tandfonline.com/loi/ystw20

Resistance spot welding of metal/carbon-fibre-reinforced plastics and applying silane coupling treatment

Kimiaki Nagatsuka, Bolyu Xiao, Lihui Wu, Kazuhiro Nakata, Shuhei Saeki, Yamato Kitamoto & Yoshiaki Iwamoto

To cite this article: Kimiaki Nagatsuka, Bolyu Xiao, Lihui Wu, Kazuhiro Nakata, Shuhei Saeki, Yamato Kitamoto & Yoshiaki Iwamoto (2017): Resistance spot welding of metal/carbon-fibre-reinforced plastics and applying silane coupling treatment, Science and Technology of Welding and Joining, DOI: 10.1080/13621718.2017.1362159

To link to this article: http://dx.doi.org/10.1080/13621718.2017.1362159

Published online: 11 Aug 2017.

SCIENCE AND TECHNOLOGY OF WELDING AND JOINING, 2017
https://doi.org/10.1080/13621718.2017.1362159

The Institute of Materials, Minerals and Mining

Taylor & Francis
Taylor & Francis Group

Resistance spot welding of metal/carbon-fibre-reinforced plastics and applying silane coupling treatment

Kimiaki Nagatsuka[a], Bolyu Xiao[a], Lihui Wu[a], Kazuhiro Nakata[a], Shuhei Saeki[b], Yamato Kitamoto[b] and Yoshiaki Iwamoto[b]

[a]Joining and Welding Research Institute, Osaka University, Osaka, Japan; [b]DENGENSHA TOA CO., LTD., Kanagawa, Japan

ABSTRACT

Dissimilar materials joining of SUS304 and carbon-fibre-reinforced plastics consisting of short fibres and thermoplastics was performed. The materials were joined by series resistance spot welding. The electrodes were pressed on the metal plate of the lap joint of metal/carbon-fibre-reinforced plastics. The SUS304 plate was heated by resistance heating, causing the thermoplastic near the interface to melt slightly because of heat conduction. SUS304 could be joined directly to carbon-fibre-reinforced polyamide and modified polypropylene, but not to polyphenylene sulphide. The joining area increased with an increase in the welding current and welding time, so did the tensile shear fracture load. Furthermore, the silane coupling agent treatment of SUS304 was highly effective in increasing the joining strength.

ARTICLE HISTORY
Received 25 April 2017
Accepted 27 June 2017

KEYWORDS
Series resistance spot welding; carbon-fibre-reinforced thermoplastic; polyamide 6; polypropylene; polyphenylene sulphide; stainless steel; dissimilar materials joining; silane coupling

Introduction

The use of multi-materials in transportation vehicles such as automobiles and railroad cars is essential for weight reduction. Carbon-fibre-reinforced plastics (CFRPs) are expected to serve as novel structural materials for transportations owing to their lightweight nature and because they show specific strengths higher than those of metals. In particular, carbon-fibre-reinforced thermoplastics (CFRTPs), which are made by adding carbon fibres (CFs) to thermoplastic matrix resins, such as polyamide (PA), polyethylene, polypropylene (PP), and polyphenylene sulphide (PPS), are highly processable and can be formed by mould-injection and hot-pressing [1]. To be able to use these CFRPs in transportation structures, various high-production-rate techniques for bonding dissimilar materials have been developed. Adhesive bonding and mechanical fastening are used conventionally for joining CFRPs [2]. However, these methods have several drawbacks. Adhesive bonding not only requires long processing times for ensuring effective bonding but also causes environmental pollution. Mechanical fastening results in increased weight and stress concentration. Direct joining by thermal fusion bonding can prevent these problems. Hence, several fusion bonding methods that use different heat sources have been investigated, such as laser joining [2,3], ultrasonic welding [4], induction heating [5], friction spot joining [6,7], friction stir welding [8], and friction lap joining [9–13]. However, resistance spot welding (RSW) has rarely been used for joining these materials [14].

RSW can join materials rapidly and at a high rate and hence is used in the manufacture of automobiles. During metal-to-metal RSW, the upper and lower plates are both of a conductive material. The electrodes are often placed on the upper and lower plates, and a welding current is passed from one electrode to the other through a welding point [15]. However, resins, which form the matrix of CFRTPs, are nonconductive. Although CFs are conductive, the CFRTPs, made by the injection moulding, are nonconductive because added CFs are cut short and the CF content is low. Therefore, it is difficult to join metal and CFRTP plates by placing electrodes on them. Therefore, the series-RSW method, wherein the electrodes are arranged only on the conductive metal side, was used for lap joining the metal to the CFRTPs.

In this method, it is possible to make the current pass only through the metal side and locally heat the metal near the electrodes through resistance heating. The passing of the current melts the matrix of the CFRTP near the joint interface by thermal conduction, resulting in its bonding. The series-RSW method for metal-to-CFRTP joining is advantageous in making a strong adhesion, because the electrodes exert a

CONTACT Kimiaki Nagatsuka nagatuka@jwri.osaka-u.ac.jp Joining and Welding Research Institute, Osaka University, 11-1, Mihogaoka, Ibaraki, Osaka 567-0047, Japan

pressure on the interface during the heating process. In addition, the method results in short joining times, causes limited deterioration of the CFRTP, has a high production rate and low equipment and running costs, can be performed using existing welding power supplies, and is easy to robotise and automate. Because this type of metal/CFRTP joining is based on the interaction between the metal surface and the molten CFRTP, the effects of the type of matrix resin as well as those of any surface treatment of the metal and the welding conditions on the joining strength are likely to be significant [3,11–13].

In this study, the authors attempted to join dissimilar materials, namely, a metal and different CFRTPs, by simple series-RSW and investigated the effects of the bonding conditions such as the welding current and time, surface treatment of the metal before joining, and matrix resin of the CFRTP on the joining properties.

Experimental methods and materials

The metallic materials used were austenitic stainless steel SUS304 plates (150 mm × 75 mm × 2 mm; Fe–18.1 mass-% Cr–8.1 mass-% Ni) with a No.2B finish (skin pass rolled after acid cleaning), which were joined with three types of injection-moulded CFRTP plates (150 mm × 75 mm × 3 mm). The CFRTP plates were composed of CFs cut short and different matrix resins (PA6, acid-modified PP, and PPS). These plates are labelled as CFRP(PA6), CFRP(PA), and CFRP(PPS). Furthermore, in addition to the as-received SUS304 plates, surface-treated SUS304 plates with a silane coupling agent were also used. The surface treatment was performed by dipping SUS304 plates into a 0.5 vol.-% aqueous solution of aminoethylaminopropyltrimethoxysilane ($C_3H_6NHC_2H_4NH_2Si(OCH_3)_3$), and then drying them.

Figure 1 shows a schematic of the experimental layout of the series-RSW process for joining the metal and CFRP plates. Table 1 shows the conditions used for the series-RSW joining of the SUS304/CFRPs plates. Dome radius-type (radius of 40 mm) Cu–Cr electrodes with a tip diameter of 8 mm were pressed on the metal side with the pressing force of 1.5 kN per electrode for electrical heating using a DC inverter-type RSW machine. Welding was performed using the DC welding currents and welding times, as shown in Table 1. Cooling with air blow was performed for 30 s after heating. To measure the temperature, thermocouples were inserted at the interface between the SUS304 and CFRP plates; the temperature histories were recorded at three points at the interface below the positive and negative electrodes as well as between them.

The series-RSW joints were cross-sectioned for macrostructural analysis using an optical microscopy (OM) system. The interfacial structure of the joints was analysed using TEM; the samples were prepared using focused ion beam milling. To evaluate the joining strength, tensile shear tests were performed at a crosshead speed of 8.3 mm s^{-1}. For each joining condition, a single specimen with the entire joint (including the entire joining area shown in Figure 1) was subjected to this test. The fracture surfaces of the test specimens were observed using OM and SEM.

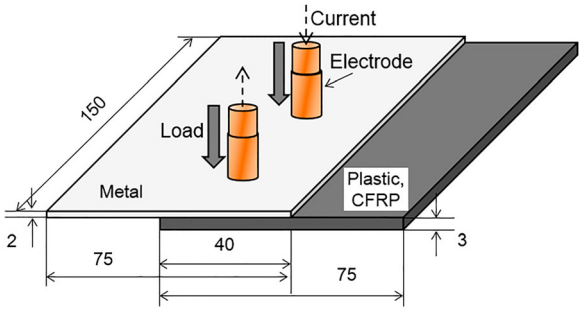

Figure 1. Schematic of experimental layout of series-RSW process for dissimilar materials joining of metal/plastic and metal/CFRPs (all dimensions in mm).

Table 1. Series-RSW conditions for forming SUS304/CFRPs joints.

Metal	CFRP	Welding current/kA	Welding time/ms
As-received SUS304	CFRP (PA6)	4–8	250–600
	CFRP (PP)	5	250
	CFRP (PPS)	5	250, 310
Silane coupling-treated SUS304	CFRP (PA6)	4–7	250

Results and discussion

Effects of welding conditions on joining strength

The direct joining of SUS304/CFRP(PA6) could be achieved under all joining conditions. Figure 2 shows the temperature history of the series-RSW process for joining the SUS304/CFRP(PA6) plates at a welding current of 5 kA and a welding time of 250 ms. As the electrical conduction process was commenced, the joint interface below the electrodes heated rapidly and then cooled. The maximum temperature at the interface exceeded the melting and thermal decomposition temperatures of PA6, the matrix resin of CFRP(PA6). There were no significant differences in the maximum temperature and cooling rate under the positive and negative electrodes. In the intermediate region between the electrodes, the maximum temperature did not reach the melting temperature of PA6. The cooling rate under the electrode was faster than that of the intermediate region, because the electrode was water cooled. With an increase in the welding current and welding time, the maximum temperature of each measured point at the interface increased. The increase in the welding current and welding time also increased the time interval during which melting and thermal decomposition could

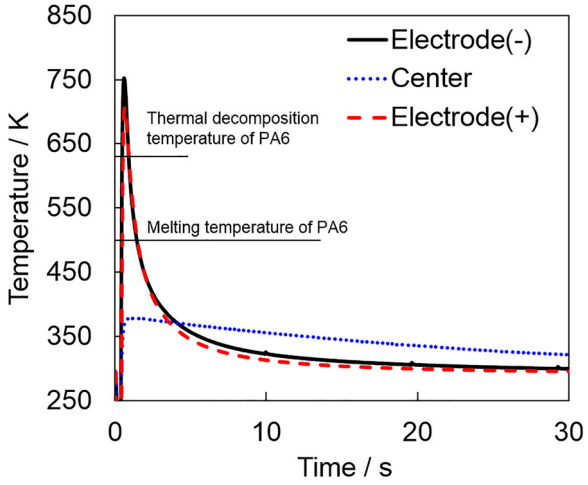

Figure 2. Temperature history of series-RSW process for forming SUS304/CFRP(PA6) joint at a welding current of 5 kA and a welding time of 250 ms.

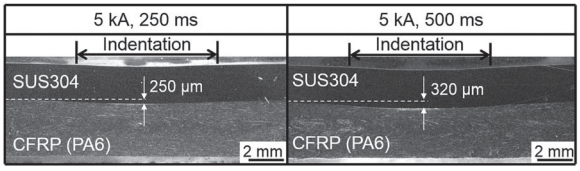

Figure 3. Cross-sectional microstructures of series-RSW SUS304/CFRP(PA6) joints formed for a welding current of 5 kA and welding times of 250 and 500 ms.

occur (i.e. the span of time over which the temperature of the matrix of CFRP(PA6) exceeded these critical temperatures).

Figure 3 shows the cross-sectional microstructures of the series-RSW SUS304/CFRP(PA6) joints formed for a welding current of 5 kA and welding times of 250 and 500 ms. These cross-sectional microstructures were taken along the direction of the shorter side of plates. The SUS304/CFRP(PA6) interface exhibited a continuous joint, and no defects such as voids were observed under electrodes. The upper SUS304 plate was deformed into a convex shape towards the lower CFRP(PA6) plate. The welding current and welding time were increased, so did the degree of deformation of the upper plate. This was probably because the CFRP(PA6) plate was softened and melted by the heating of the upper SUS304 plate and was extruded to the surrounding area by the SUS304 plate, which was pressed by the electrode.

Figure 4 shows a bright-field TEM image of the interface of the series-RSW SUS304/CFRP(PA6) joint. The SUS304/CFRP(PA6) joint was formed by the joining of the PA6 matrix of the CFRP and SUS304. An amorphous layer, which would be of Cr oxide and/or the hydroxide of SUS304, was observed between PA6 and SUS304.

Figure 5 shows the effects of the (a) welding current and (b) welding time on the tensile shear fracture

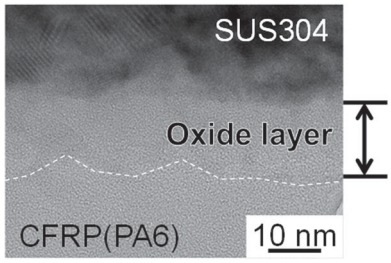

Figure 4. Bright-field TEM image of interface of series-RSW SUS304/CFRP(PA6) joint formed for a welding current of 5 kA and a welding time of 250 ms.

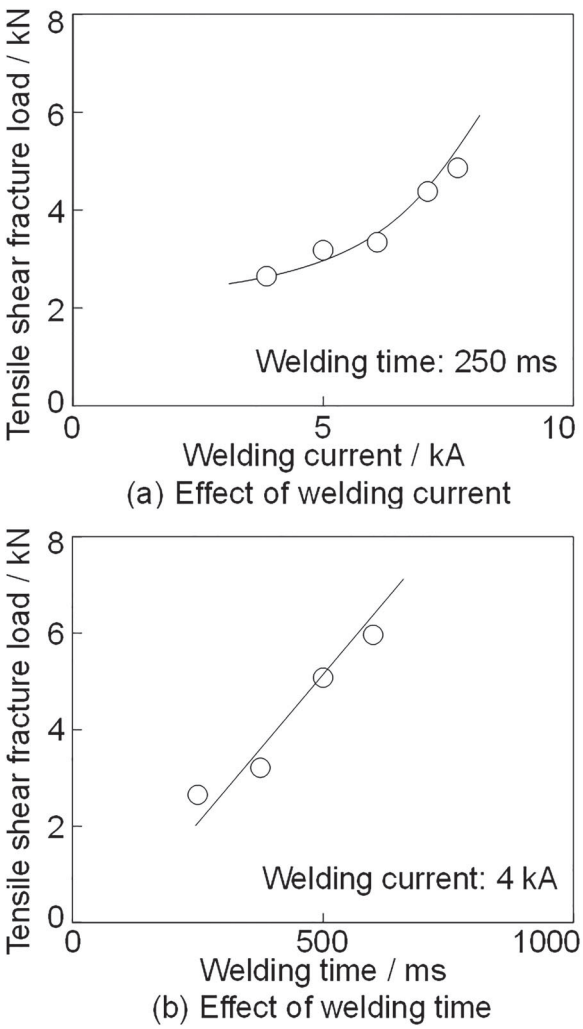

Figure 5. Effects of (a) welding current and (b) welding time on tensile shear fracture load of series-RSW SUS304/CFRP(PA6) joints.

load of the series-RSW SUS304/CFRP(PA6) joints. The tensile shear fracture load increased with an increase in the welding current and welding time. Furthermore, with an increase in the welding time, the tensile shear fracture load of the joint increased linearly, while in the case of the welding current, it increased quadratically. This is because the degree of resistance heating is proportional to the welding time and to the square of the welding current [15]. Macroscopically, the fracturing of the joints occurred at the joint interface under

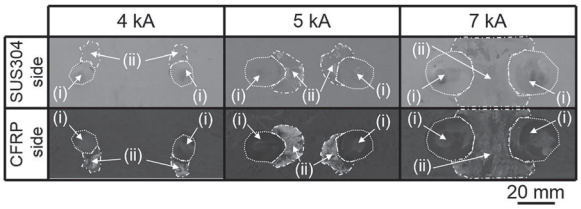

Figure 6. Matching pairs fracture surfaces with the effective joining area (region (i)) and the discoloured area (region (ii)) of series-RSW SUS304/CFRP (PA6) joints formed at welding currents of 4, 5, and 7 kA, at a welding time of 250 ms.

every condition. Figure 6 shows the matching pairs fracture surfaces with the effective joining area (region (i)) and the discoloured area (region (ii)) of series-RSW SUS304/CFRP (PA6) joints formed at welding currents of 4, 5, and 7 kA, at a welding time of 250 ms. In all the joints, a melted area was observed on the CFRP(PA6) side, and residual CFRP(PA6) was observed on the SUS304 side. There were no significant differences in the sizes of the melted areas on the sides of the positive and negative electrodes. Although, macroscopically, these joints exhibited interfacial fracturing, it was evident that the fracturing of the CFRP(PA6) plate also occurred under every condition. The melted areas of CFRP(PA6) could be classified into regions (i) and (ii), with the fracture modes of these regions being distinctly different.

In region (i), the fracture surface of both the SUS304 side and the CFRP(PA6) side was rough, and the exposed CFs could be observed; hence, this region exhibited ductile fracturing of CFRP(PA6). Region (i) can be considered the effective joining region. In contrast, the surface of residual CFRP(PA6) on SUS304 in region (ii), which had turned yellowish brown, was flat and fractured at a part of the void part. This region exhibited brittle fracturing. Region (ii) can be considered the region where the thermal degradation of CFRP(PA 6) occurred; this region did not contribute significantly to the joint. These melted areas increased in size with an increase in the welding current and welding time. It is likely that, with the increases in the welding current and welding time, the effective joining area increases, resulting in an increase in the tensile shear fracture load of the corresponding joint.

Effect of treatment with silane coupling agent on joint formation

Figure 7 shows the tensile shear fracture load of as-received SUS304 and silane coupling agent-treated SUS304/CFRP(PA6) joints formed at welding currents of 4–7 kA and a welding time of 250 ms. For all the welding currents, the joints formed using the SUS304 plates treated with the silane coupling agent showed significantly higher fracture loads than did those formed using the as-received SUS304 plates. The tensile shear

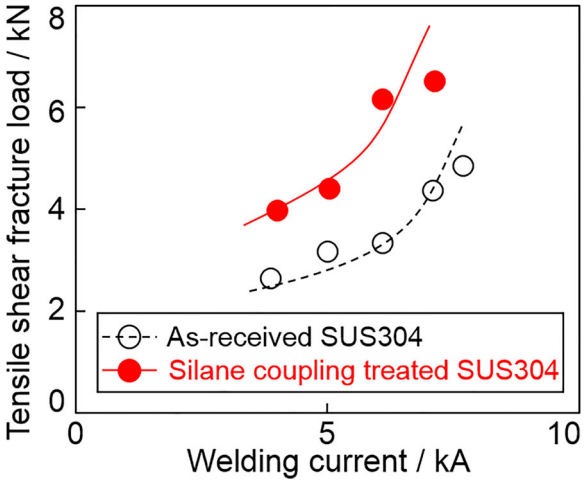

Figure 7. Tensile shear fracture load of as-received SUS304 and silane coupling agent-treated SUS304/CFRP(PA6) joints formed at welding currents of 4–7 kA and a welding time of 250 ms.

fracture load increased with the welding current even in the case of the treated SUS304 plates. Furthermore, these joints fractured macroscopically at the joint interface with the residual CFRP(PA6) on SUS304 side. The reason the fracture load of the SUS304/CFRP(PA6) joints increased after the treatment with the silane coupling agent would be that a chemical bond was formed at the joint interface. It has been proposed that the mechanisms of fusion bonding of metal/CFRTP joints are an anchor effect, the Van der Waals forces and the formation of hydrogen bonds between the oxide layer on metal surface and the polar functional groups in the resin of the CFRP [3,11–13]. SUS304 plates with flat surfaces were used in this study to limit the anchor effect. Thus, in the case of these metal plates with flat surfaces, the primary joining mechanism is likely to be hydrogen bonding. After the treatment with the silane coupling agent, a silane coupling layer is formed on the metal plate surface through covalent bonding with the metal oxide layer. Because the amino group (NH_2), which is a polar functional group, was present in the silane coupling layer, it is likely that hydrogen bonds formed between this group and the amide group (CONH) in the PA6 matrix of CFRP(PA6). Furthermore, it is possible that the carboxyl group (COOH) at the ends of the PA6 molecular chains as well as at the ends formed by the cleavage of the molecular chain owing to thermal decomposition formed covalent bonds such as amide bonds with the amino group in the silane coupling layer [13]. This is the reason for the increased strength of the joints formed between SUS304 and CFRP(PA6) after the treatment with the silane coupling agent.

Effect of matrix resin on joint formation

Figure 8 shows the tensile shear fracture loads of the series-RSW joints formed between the SUS304 and

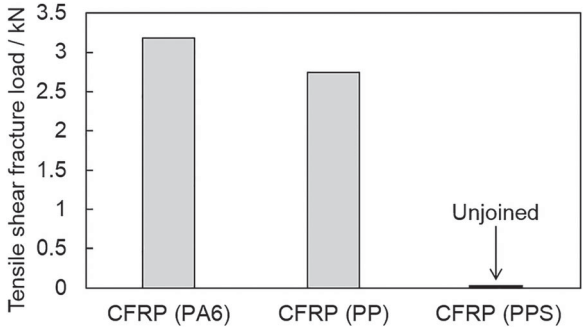

Figure 8. Tensile shear fracture loads of series-RSW SUS304/various CFRP joints formed for a welding current of 5 kA and a welding time of 250 ms.

the various CFRP plates for a welding current of 5 kA and a welding time of 250 ms. The tensile shear fracture load was approximately 3.2 kN for the CFRP(PA6) joint and approximately 2.7 kN for the CFRP(PP) joint; a joint could not be formed using the CFRP(PPS) plate. The joints fractured at the SUS304/CFRP interface, and their fracture surfaces could also be classified into an effective bonding region (region (i)) and a region formed by the thermal decomposition of the CFRP (region (ii)) (see Figure 6). The melted areas of these joints, shown on the fractured surfaces, could be arranged in the following decreasing order in terms of size: CFRP(PP), CFRP(PA6), and CFRP(PPS). As the melting points of the matrix resins of the CFRPs are 436 K (for PP), 498 K (for PA6), and 551 K (for PPS), it can be concluded that when a material having a high melting point is used as the matrix, the melted area of the CFRP is smaller for the same heat input. The tensile shear fracture load of the CFRP(PA6) joints was higher than that of the CFRP(PP) joints. Although these joints macroscopically fractured at the interface, the base CFRP materials were also fractured. The differences in the fracture loads of the two types of joints can be attributed to the differences in the strengths of CFRP(PA6) and CFRP(PP). The tensile strength of CFRP(PA6) was about 110 MPa, and that of CFRP(PP) was about 70 MPa. Although the matrix resin melted for all the CFRPs, CFRP(PPS) could not be joined with SUS304. This was probably owing to the absence of polar functional groups in the resin. These polar groups contain atoms with different electronegativities. In the case of PA6, the O, N, and H atoms in the amide (CONH) group are polarised as O ($-\delta$), N ($-\delta$), and H ($+\delta$) owing to the differences in their electronegativities. Moreover, metal oxides are also polarised similarly. In this study, an amorphous Cr oxide and/or hydroxide layer was detected at the SUS304/CFRP(PA6) interface; thus, in the oxide/hydroxide layer, these elements were polarised as Cr ($+\delta$) and O ($-\delta$). Hence, these materials (SUS304 and CFRP(PA6)) were joined by Coulombic forces (hydrogen bonding) between the oxide/hydroxide layer on the metal and the polar group in the resin [10–12]. On the other hand, PP does not contain a polar functional group. However, in the acid-modified PP sample used in this study, a polar functional group is present, owing to the acid treatment. Therefore, this polar group formed hydrogen bonds with the metal oxide/hydroxide, resulting in joint formation. Finally, PPS is a non-polar resin and does not contain any polarised atoms. Thus, in this case, only the Van der Waals forces and the anchor effect occurred at the SUS304/CFRP(PPS) interface. As a result, a SUS304/CFRP(PPS) joint could not be formed.

Conclusions

The joining of SUS304 and CFRTPs was attempted through series RSW, and the effects of the joining conditions such as the welding current and time, treatment with a silane coupling agent before joint formation, and type of matrix resin of the CFRTP on the joining properties were investigated.

(i) Direct joining between SUS304 and carbon-fibre-reinforced polyamide 6 could be accomplished for welding currents of 4–8 kA and a welding time of 250–600 ms.
(ii) The SUS304/carbon-fibre-reinforced polyamide 6 interface under the electrodes heated immediately during the resistance heating process, with its temperature exceeding the melting point of polyamide 6, and then cooled rapidly. A layer of an amorphous oxide or hydroxide of SUS304 was observed at the interface. The SUS304/carbon-fibre-reinforced polyamide 6 joint was formed because of bonding between this layer and the matrix resin of carbon-fibre-reinforced polyamide 6.
(iii) The joining area increased with the welding current and welding time, so did the tensile shear fracture load.
(iv) The surface treatment of SUS304 with a silane coupling agent increased the joining strength of the SUS304/carbon-fibre-reinforced polyamide 6 joint.
(v) The joining of SUS304/carbon-fibre-reinforced polyamide 6 and SUS304/carbon-fibre-reinforced modified PP was achieved but that of SUS304/carbon-fibre-reinforced PPS was not.

Disclosure statement

No potential conflict of interest was reported by the authors.

Funding

This work was partly supported by JSPS KAKENHI Grant Number JP 16K18247.

References

[1] Fu SY, Lauke B, Mäder E, et al. Tensile properties of short-glass-fiber- and short-carbon-fiber-reinforced polypropylene composites. Compos Part A-Appl S. 2000;31:1117–1125.

[2] Katayama S, Kawahito Y. Laser direct joining of metal and plastic. Scr Mater. 2008;59:1247–1250.

[3] Hino M, Mitooka Y, Murakami K, et al. Effect of aluminum surface state on Laser joining between 1050 aluminum sheet and polypropylene resin sheet using insert materials. Mater Trans. 2011;52:1041–1047.

[4] Balle F, Wagner G, Eifler D. Ultrasonic spot welding of aluminum sheet/carbon fiber reinforced polymer – joints. Mater Werks. 2007;38:934–938.

[5] Mitschang P, Velthuis R, Emrich S, et al. Induction heated joining of aluminum and carbon fiber reinforced nylon 66. J Thermoplast Compos Mater. 2009;22:767–801.

[6] Amancio-Filho ST, Bueno C, dos Santos JF, et al. On the feasibility of friction spot joining in magnesium/fiber-reinforced polymer composite hybrid structures. Mater Sci Eng A. 2011;528:3841–3848.

[7] Yusof F, Miyashita Y, Seo N, et al. Utilising friction spot joining for dissimilar joint between aluminium alloy (A5052) and polyethylene terephthalate. Sci Technol Weld Join. 2012;17:544–549.

[8] Ratanathavorn W, Melander A. Dissimilar joining between aluminium alloy (AA 6111) and thermoplastics using friction stir welding. Sci Technol Weld Join. 2015;20:222–228.

[9] Liu FC, Nakata K, Liao J, et al. Reducing bubbles in friction lap welded joint of magnesium alloy and polyamide. Sci Technol Weld Join. 2014;19:578–587.

[10] Nagatsuka K, Yoshida S, Tsuchiya A, et al. Direct joining of carbon-fiber-reinforced plastic to an aluminum alloy using friction lap joining. Composites Part B: Eng. 2015;73:82–88.

[11] Liu FC, Liao J, Gao Y, et al. Effect of plasma electrolytic oxidation coating on joining metal to plastic. Sci Technol Weld Join. 2015;20:291–296.

[12] Nagatsuka K, Kitagawa D, Yamaoka H, et al. Friction lap joining of thermoplastic materials to carbon steel. ISIJ Int. 2016;56:1226–1231.

[13] Nagatsuka K, Tanaka H, Xiao B, et al. Effect of silane coupling treatment on the joint characteristics of friction lap joined Al alloy/CFRP. Q J Jpn Weld Soc. 2015;33:317–325.

[14] Nagatsuka K, Xiao B, Wu L, et al. Dissimilar materials joining of metal/carbon fiber reinforced plastic by resistance spot welding. Q J Jpn Weld Soc. 2016;34:267–273.

[15] Pouranvari M, Marashi SPH. Critical review of automotive steels spot welding: process, structure and properties. Sci Technol Weld Join. 2013;18:361–403.